Proceedings of the 16th IAHR International Symposium on Ice
Dunedin, New Zealand, 2nd–6th December 2002
International Association of Hydraulic Engineering and Research

IN SITU SEA ICE STRESSES IN THE WESTERN ARCTIC DURING THE WINTER OF 2001-2002

Jackie Richter-Menge[1], Bruce Elder[1], Kerry Claffey[1], Jim Overland[2] and Sigrid Salo[2]

ABSTRACT
An array of 9 autonomous drifting buoys was deployed in the Canadian Beaufort Sea in the September 2001. These buoys measured ice stress and position, sending data back to the mainland, via satellite, for analysis. The array was designed to study the development of stresses as the wind drives the sea ice cover against a coastline and to investigate the spatial variability of ice stress. In this paper, we will present the initial results from the buoy array, describing the characteristics of ice drift and ice stress during the measurement period.

INTRODUCTION
Recent efforts have been made to significantly increase the spatial resolution of sea ice dynamics models, using both continuum-based (e.g. Hibler, 2001; Zhang et al., 1999; Hunke and Zhang 1999) and discrete element models (e.g. Hopkins, 1996). For instance, the most recent update of the US Navy's operational model looks to employ an 18-km grid size. Coupled with the goal of developing a high resolution sea ice model is the need for establishing a more detailed understanding of the processes governing ice motion (Overland et al., 1995). In particular, we are interested in exploring the application of direct measurements of ice stress and deformation in the development and validation of the rheological component of sea ice dynamics models. Currently, the ice rheology is evaluated indirectly by comparing modeled and observed ice drift tracks. The compressive strength of the ice cover, a fundamental parameter in the rheological equation, is adjusted in the model to achieve good agreement of the ice motion.

During the recent SIMI (Overland et al., 1998; Richter-Menge and Elder, 1998) and SHEBA (Richter-Menge et al., in press) experiments we used a combination of in situ stress measurements, position buoys, and, when available, satellite-derived ice motion products to study the relationship between internal ice stress and deformation. During SIMI, we focused on the distribution of stress within a single multi-year ice floe. We observed that stresses measured at different sites on a single floe varied in magnitude, but showed a strong temporal correspondence. This suggests that all of the sites were

[1] ERDC - Cold Regions Research and Engineering Laboratory, Hanover, NH, USA
[2] NOAA- Pacific Marine Environmental Laboratory, Seattle, WA. USA

reacting to the same general loading event, rather than events specific to each site. This is consistent with the characteristics of a granular plastic, where the fundamental component, in this case, is the ice floe. The system's plasticity is established by the interaction of the floes, which move together in aggregate plates separated by narrow sliplines. Satellite-derived ice motion velocity data show that deformation occurs along line that are often ~40-50 km apart and can extend for hundreds of kilometers.

During SHEBA we observed the temporal correspondence of ice stress in floes that were separated by as much as 15 km. Further, we found that using the average of the ice-motion-induced stress at the different sites, rather than any specific, individual site, provided a better representation of the regional stress activity. Selected individual case studies provided direct confirming evidence that regional-scale ice dynamics is primarily a function of coastal geometry and sustained, large-scale wind direction and magnitude.

This paper describes the continuation of our efforts to provide direct measurements of ice stress and deformation for the development and evaluation of sea ice dynamics models. More specifically, we deployed another array of buoys equipped with instruments to measure stress and position. This array was purposefully located in roughly the same region as the SHEBA and SIMI arrays. It was our interest to observe the ice cover loading conditions that were consistent with the SHEBA and SIMI experiments. The unique features of this array were that it covered a larger region (200 km) and that it was oriented along a line. These characteristics were selected to provide insight on the areal extent of the aggregate behavior of the ice pack and to test the hypothesis that, during a loading event, stress propagates outward from the coast, producing a compressional wave. Here we present the early results of our experiment, describing the ice drift and average ice stress during the measurement period.

BUOY ARRAY

The buoy array was deployed in late September 2001, in the Canadian sector of the Beaufort Sea (Figure 1). The *CCGS Sir Wilfrid Laurier* served as the base of operation for the deployment. A total of 9 autonomous data collection sites made up the array. Five of the buoys were spaced approximately 50 km apart, along a 200-km-long line that generally ran Northwest-Southeast. The site closest to shore was located inside the edge of the perennial ice zone, approximately 360 km from the coastline. Ice charts indicate that, at this time, the ice edge in the region of our deployment was located at approximately 72°N. The remaining 4 buoys were deployed to form a 10-km^2 box around the site that fell at the center of this line.

Each of the buoys was instrumented with a stress sensor (Cox and Johnson, 1983), to measure the internal ice stress, and GPS, to provide information on the position. The stress sensors were located near the surface of the ice cover, at an average depth of 39 cm. The average ice thickness at the deployment sites was 190 cm, ranging widely from 49 cm to 413 cm. The buoys also collected data on the temperature at the snow/ice interface and the air pressure near the surface of the ice cover. At the center site, we deployed additional buoys equipped with instruments to measure meteorological conditions and the ice mass balance (Perovich and Elder, 2001). All of the buoys were equipped with a satellite transmitter, allowing all data to be transmitted back to the mainland for archiving and analysis.

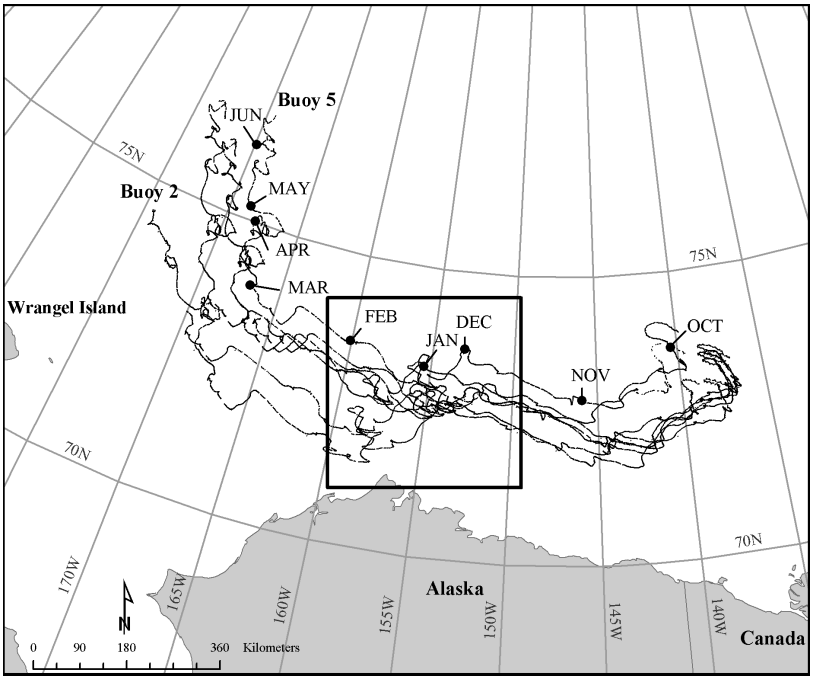

Figure 1: Drift tracks of buoys installed in late September 2001

RESULTS

Drift tracks

The drift tracks of the individual buoys are presented in Figure 1. Month markers for buoy 5 are provided to give a general sense of the relative rate of movement. In general, the buoy tracks are consistent with the general circulation pattern in the region of the Arctic, which is dominated by the Beaufort Gyre. The formation of the Beaufort Gyre reflects predominant wind and ocean currents.

A more detailed look at the drift tracks reveals that after installation in late September, all of the buoys moved rapidly westward during the months of October and November. Overall, the buoys located further south moved further west during this period. This likely reflects the differences in the relative compactness and thickness of the ice cover. When the buoys were installed there was open water between the coast and perennial ice zone. Ice charts indicate this region was ice-covered by mid-October. However, since it was new ice it was significantly thinner than the pack ice and, hence, easier to deform. The westward movement of the buoys continued in December, albeit at a slower rate. In late December and early January, the buoys stalled north of Barrow, Alaska. Once the generally westward movement resumed, there was an increase in the rate of movement. Late in February, the northern component of drift began to increase and, by the end of the month, dominated the drift direction. This change in the dominant direction reflects the increased influence of the Siberian coast, including Wrangel Island. As the buoys moved northward, their rate of movement again slowed. There was another period when the buoys appeared to stall in late March and early April.

Ice stress

The time series for the internal ice stress is presented in Figure 2. As initially discussed in Richter-Menge and Elder (1998), the stress sensors used in our experiments do not distinguish between different sources of stress. Under winter conditions in the central Arctic, there are two primary sources of stress: changes in the ice temperature and ice motion. We are primarily interested in ice-motion-induced stresses for the purposes of sea ice dynamics model development and evaluation. Hence, it is necessary to isolate this component of the total stress signal. Richter-Menge and Elder demonstrated, that, under winter conditions in the central Arctic, ice-motion-induced stresses can be estimated by subtracting the primary principal stress from the secondary principal stress ($\sigma_1 - \sigma_2$). The stress presented in Figure 2 was obtained using this approach. Further, we use the average of the ice-motion-induced stress measured at the different sites in our analysis, rather than any specific, individual site, because the average better represents the regional stress activity (Richter-Menge et al, in press).

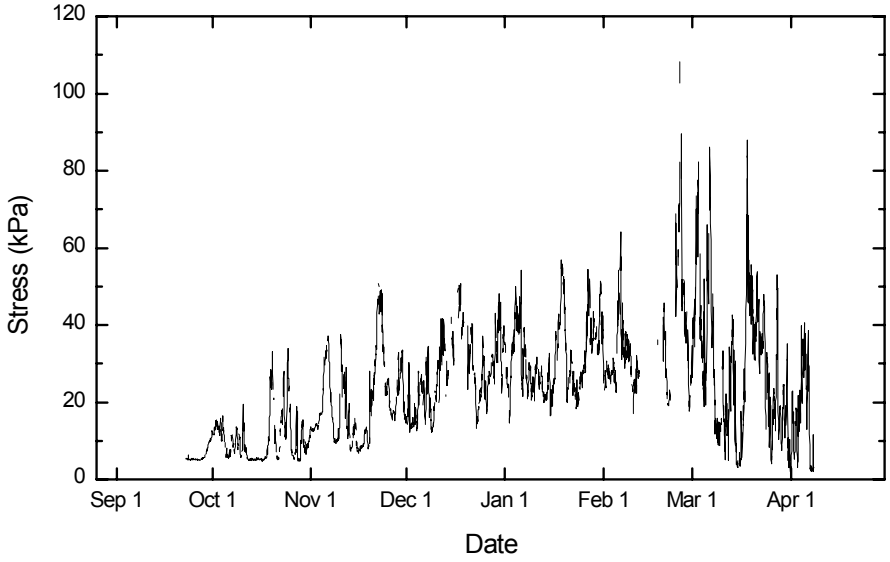

Figure 2: Time series of the internal ice stress between 22 September 2001 and 8 April 2002.

The general characteristics of the stress time series are consistent with our earlier findings in SIMI (Richter-Menge and Elder, 1998) and SHEBA (Richter-Menge et al, in press). This result is expected since, as we have previously mentioned, we purposefully located this array in the same region as the SIMI and SHEBA arrays. One of the most pronounced features of the stress signal is its episodic nature. Sustained periods of relatively high stress are called stress events. Individual stress events are comprised of both rapid and longer-duration changes in the magnitude of the stress. The large and rapid changes in the stress are associated with the formation of ridges, leads, and rubble fields. These changes in stress happen on the order of hours and give the stress signal its spiky appearance. Underlying the rapid changes in the stress is a more gradual increase and, then, decrease in the stress. These longer-duration changes happen over a time period that is on the order of days, coincident with storm patterns.

Beginning in mid-November, the sequence of stress events appear linked by a gradual but marked increase in the underlying stress. Up until mid-November, between stress events the stress returns to near zero. By the beginning of March the baseline stress has increased to 20 kPa. At this point, there are some dramatic variations in the magnitude of the high frequency component of the stress signal, as large as 100 kPa. By 10 March, the underlying stress returns to near-zero, again, between stress events. The dramatic changes in the high frequency component of the stress signal continue until the beginning of April.

The overall magnitude of the average internal ice stress measured during this experiment is slightly higher than measured during SHEBA. This difference is due mainly to the contribution from the gradual increase of the underlying stress observed during this experiment. During SHEBA, from 1 November 1997 to 1 April 1998, the average peak stress during individual events typically ranged from 30 to 40 kPa. There was one extreme event at the beginning of February 1998, when the average peak stress ranged as high as 60 kPa. In this experiment the average peak stress typically ranged from 30 kPa to 60 kPa. Peaks of 60 kPa were achieved when the baseline stress had increased to 20 kPa. During the first half of March 2002, there was a period when peak average stresses were approximately 80 kPa and, once, was as high as 100 kPa.

DISCUSSION

Data from the SIMI and SHEBA experiments suggested that the material behavior of the sea ice cover was consistent with the characteristics of a granular plastic. While the ice cover is made of individual ice floes, they move together as aggregate plates. Deformation of the ice cover is concentrated along sliplines. In the experiment initiated in September 2001, we obtained a detailed perspective of the regional movement of the sea ice cover, over distances of 200 km. Early looks at the data provide strong, consistent evidence that there is significance coherency in the ice pack over this distance. A portion of the drift tracks for buoys 2 and 5 is presented in Figure 3, to illustrate this point. These buoys had the greatest separation distance: on 1 December 2001, they were separated by 109 km; on 1 January 2002, they were 162 km apart, and on 1 February, they were 192 km apart. While there are obviously differences in the details of these buoy tracks, the general pattern of movement is clearly consistent. For instance, at the end of November and the beginning of December, both buoys move North, then West, and then South, in concert. At the beginning of January, both buoy tracks show a consistent, intricate pattern, which includes a clockwise loop elongated in the East-West direction. Clearly, the components of the sea ice cover in this region are moving as an aggregate.

Combined, the overall drift track and the time series of the average internal ice stress provide further detailed insight on the relationship between ice stress and deformation. Recall that between mid-November and the beginning of March, there was a gradual, but consistent increase in the underlying average internal ice stress, from near zero to 20 kPa. It is our hypothesis that this change indicates an increase in the compressive failure strength of the ice cover. Further, we feel that mechanical thickening of the ice cover played a significant role in the increase of the compressive failure strength.

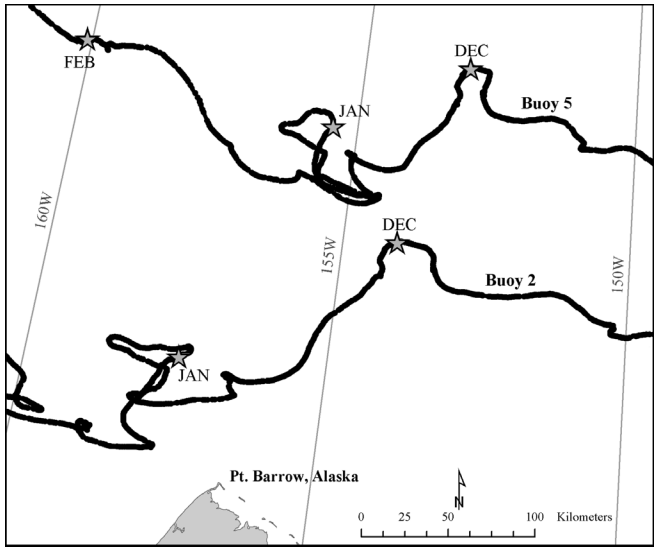

Figure 3: Detailed map of drift track for buoys 2 and 5, illustrating the regional coherency in ice deformation. The region covered in this figure corresponds to the box shown in Figure 1.

It is generally accepted that the strength of the sea ice cover is a function of the ice concentration and the ice thickness. After 1 November, ice charts show that this region of the Arctic was completely ice covered and remained so through at least April. Therefore, over the this period changes in the ice concentration where constant, at approximately 100 %, and did not contribute to a strengthening of the ice cover. The thickness of the ice cover changes as a result of thermodynamic (growth and ablation) and dynamics (ridge and lead formation) processes. The thermodynamic contribution plays a more significant role in strengthening of the sea ice cover early in the season, when there is a significant amount of young ice. By 1 January, much of the sea ice cover has nearly reached its maximum thickness. Beyond this point, mechanical thickening is left to account for the significant observed increase in the compressive failure of the ice cover.

Based on the results from SIMI and SHEBA, we feel that the predominant westward drift of the ice cover from November to March would provide the conditions necessary for a significant the mechanical thickening of the ice cover. The westerly drift of the ice cover moves the buoys towards the coastal boundary presented by Siberia and creates a persistent compressive loading. This situation gives rise to dramatic failure events, with lead and ridge systems reaching far offshore, into the central pack. With each failure event the ice pack thickens and the overall strength of the ice cover increases. We observed these effects during SHEBA, in early February when the ice camp had reached a longitude of 155ºW. At this point, the average internal ice stress measured during the SHEBA experiment also exhibited a gradual increase in the underlying component. In the current experiment, the buoys exhibited a much higher rate of westerly movement early on, reaching a longitude of 153ºW by the beginning of December.

SUMMARY AND FUTURE WORK

The consistency between the ice drift pattern and the general characteristic of the internal ice stress between this experiment and SIMI and SHEBA is encouraging. It reinforces our fundamental working assumption that direct measurements of ice stress and deformation can be used in the development and evaluation of sea ice dynamics models, in particular, the models' rheological component. Differences in the details of the drift pattern and the internal ice stress serve to confirm the significant challenge associated with realizing this objective. Further encouragement lies in the observation that the magnitude of the observed internal ice stress is comparable to the compressive ice strength used in models. Recent ice dynamic model studies have assumed that the ice compressive strength is on the order of 10 kPa (Hunke and Dukowicz, 1997; Zhang and Hibler, 1997).

Combining the current data set with those obtained during SIMI and SHEBA provides important insights on the detailed behavior of the ice cover, necessary to establish the bridge between models and direct measurements. Unique observations from the early look at the data from this most recent experiment are:

- The mechanical thickening of the sea ice cover played a significant role in increasing the overall strength of the ice cover, by approximately 20 kPa
- The movement of the sea ice cover exhibited coherency of distances of 150–200 km.

Much work remains in the analysis of this new data set, to confirm, extend, and apply these insights. Specifically, we will more closely consider the combined time series of the ice drift and average internal ice stress. Individual buoy records will also be analyzed to determine the variations in ice motion and ice stress at a high resolution and to see whether we can observe the development of a compressional wave in the sea ice cover during a stress event. Wind forcing fields and satellite-derived ice motion products will be added to the pool of observations. In the end, from SIMI, SHEBA and the current experiment, we will produce an archival data set of ice stress and deformation that can be used for the development and evaluation of sea ice dynamic models.

ACKNOWLEDGEMENTS

This work was sponsored by the US Office of Naval Research, High Latitudes Dynamics Program. Special thanks goes to Dennis Conlon, ONR, and Marty Bergmann, Canadian Department of Fisheries and Oceans, for arranging for our passage on the *CCGS Sir Wilfrid Laurier* and to the crew of the *CCGC Sir Wilfrid Laurier* for their outstanding logistical support.

REFERENCES

Cox, G.F.N. and J.B. Johnson. Stress measurements in ice. *USA Cold Regions Research and Engineering Laboratory,* CRREL Rep. (1983) 83–23.

Hibler, W.D., III. Modeling the formation and evolution of oriented fractures in sea ice. *Annals of Glaciology 33*: 157–164 (2001).

Hopkins, M.A. On the mesoscale interaction of lead ice and floes. *Journal of Geophysical Research 101*(C8): 18,315–18,326 (1996).

Hunke, E.C., and J.K. Dukowicz. An elastic-viscous-plastic model for sea ice dynamics. *Journal of Physical Oceanography 27*(9): 1849–1867 (1997).

Hunke, E.C. and Y. Zhang. A comparison of sea ice dynamics models at high resolution. *Mon. Weather Rev. 127*: 396–408 (1999).

Overland, J.E., S.L. McNutt, S. Salo, J. Groves and S. Li. Arctic sea ice as a granular plastic. *Journal of Geophysical Research 103*: 21845–21867 (1998).

Overland, J.E., B.A. Walter, T.B. Curtin and P. Turet. Hierarchy and sea-ice mechanics: A case study from the Beaufort Sea. *Journal of Geophysical Research 100*: 4559–4571 (1995).

Perovich, D.K and B.C. Elder. Temporal evolution of Arctic sea-ice temperature, Annals of Glaciology *33*: 207–211 (2001).

Richter-Menge, J.A. and B.C. Elder. Characteristics of pack ice in the Alaskan Beaufort Sea. *Journal of Geophysical Research 103*(C10): 21,817–21,829 (1998).

Richter-Menge, J.A., L.S. McNutt, J.E. Overland and R. Kwok. Relating Arctic Pack Ice Stress and Deformation Under Winter Conditions. *Journal of Geophysical Research*, in press.

Zhang, J.L., and W.D. Hibler III. On an efficient numerical method for modeling sea ice dynamics. *Journal of Geophysical Researc*h 102(C4): 8691– 8702 (1997).

Zhang, Y, W. Maslowski and A. J. Semtner. Impact of mesoscale ocean currents on sea ice in high-resolution Arctic ice and ocean simulations. *Journal of Geophysical Research 104*: 18409–18429 (1999).